



HAL
open science

Functionalization of cyclic olefin copolymer substrates with polyethylene glycol diacrylate for the in situ synthesis of immobilized nanoparticles

Josiane Saadé, Nina Declas, Pedro Marote, Claire Bordes, Karine Faure

► To cite this version:

Josiane Saadé, Nina Declas, Pedro Marote, Claire Bordes, Karine Faure. Functionalization of cyclic olefin copolymer substrates with polyethylene glycol diacrylate for the in situ synthesis of immobilized nanoparticles. *Journal of Materials Science*, 2017, 52 (8), pp.4509-4520. 10.1007/s10853-016-0696-8 . hal-01515322

HAL Id: hal-01515322

<https://hal.science/hal-01515322>

Submitted on 23 Jul 2020

HAL is a multi-disciplinary open access archive for the deposit and dissemination of scientific research documents, whether they are published or not. The documents may come from teaching and research institutions in France or abroad, or from public or private research centers.

L'archive ouverte pluridisciplinaire **HAL**, est destinée au dépôt et à la diffusion de documents scientifiques de niveau recherche, publiés ou non, émanant des établissements d'enseignement et de recherche français ou étrangers, des laboratoires publics ou privés.

Functionalization of cyclic olefin copolymer substrates with polyethylene glycol diacrylate for the in situ synthesis of immobilized nanoparticles

Josiane Saadé, Nina Declas, Pedro Marote, Claire Bordes, and Karine Faure

Université de Lyon, CNRS, Université Claude Bernard Lyon 1, ENS de Lyon, Institut des Sciences Analytiques, UMR 5280, 5 rue de la Doua, F-69100 VILLEURBANNE, France

karine.faure@isa-lyon.fr

1 1 Introduction

2 Microfluidic systems are actually in development owing to their significant advantages: the
3 reduction of solvent consumption and the faster analysis. Furthermore, the implementation of
4 nanoparticles as novel stationary phase in microchips could in the future offer enhanced
5 chromatographic performances as shown by Knox and other authors [1-4]. Up to now, the smallest
6 particles in conventional columns present 1.7 μm as diameter [5].

7 Usually, polymers colloids are made from emulsion polymerization, like miniemulsion, which
8 could be thermally [6] or photochemically initiated [7, 8]. UV irradiation approach allows
9 polymerization in enclosed system in few minutes and at room temperature without stirring.
10 Thereby, the synthesis of hexyl acrylate nanoparticles (C_6) was executed by emulsion radical
11 polymerization. Miniemulsion composition was previously optimized by central composite design
12 and C_6 nanoparticles, obtained after photopolymerization was monodisperse with a diameter
13 inferior to 200 nm which could be used as new stationary phase [9]. To anchor nanoparticles into
14 microchips, the polymerization of miniemulsion is initiated in-situ by the abstraction of hydrogen
15 from the surface.

16 Photoinitiator type II like benzophenone (BP), react by hydrogen abstraction from the surface and
17 form ketyl (semipicanol) free radical and an alkyl free radical [10-14]. Benzoin methyl ether
18 (BME) is a type I photoinitiator used in polymerization to generate free radicals and as it has been
19 showed by Ladner et al.[15], it can react with COC by abstracting hydrogen from the surface. This

20 process, allows the photografting of acrylate nanoparticles on COC surface under UV irradiation
21 at 365 nm. Wang et al. [16, 17] reported the photografting of methyl methacrylate/ 1,2-
22 divinylbenzene (MMA/DVB) emulsion, initiated by UV-irradiation on polypropylene (PP) film.
23 Nanoparticles diameter is about 30 nm and 60 nm, anchored by covalent bond on PP film, using
24 benzophenone as photoinitiator. Furthermore, the formation of group dormant permits a growth of
25 the multilayer graft nanoparticles. The anchorage of nanoparticles into microchips depends on the
26 nature of the material. A variety material have been used, for different applications, such silicon :
27 polydimethylsiloxane (PDMS), glass, quartz, thermoplastic materials like poly
28 (methylmethacrylate) (PMMA) and polyolefin such as polyethylene (PE), polypropylene (PP) and
29 cyclic olefin copolymer (COC). COC is one of the most widely used because of its resistance to
30 many organic solvents, its transparency below
31 300 nm [18, 19] and optical detection.

32 Preliminary synthesis of spherical C₆ nanoparticles on COC chips revealed the need of surface
33 modification. Hydrophobic nature of the material seems disturbing miniemulsion stability during
34 in-situ photopolymerization. To promote the approach and the anchorage of spherical
35 nanoparticles to the surface, many methodologies of COC surface modification are proposed using
36 physical or chemical coating [20]. In literature, Roy et al. [21, 22] discussed the physical COC
37 coating by plasma treatment using argon and argon-oxygen to enhance hydrophilicity and increase
38 wettability of COC surface. Both treatments showed an increase of wettability and roughness, but
39 compared to argon plasma, oxygenated-plasma increased more effectively the wettability of COC
40 surface. Other approaches including UV/ozone oxidation treatment [23], dynamic coating with
41 hydrophilic polymers [24], covalent grafting method by aryldiazonium salts [25] and UV-
42 photografting of hydrophilic polymers [26, 27] are used for COC microchannels modification.

43 UV-photografting of hydrophilic polymers is a common strategy for modification of
44 polydimethylsiloxane (PDMS) [28-30] and thermoplastic materials [20, 31] : polyethylene films
45 [13, 32-35], polypropylene substrates [16, 17, 36-40], polycarbonateurethane [41] and cyclic olefin
46 copolymer (COC) [15, 26, 42-47]. UV-photografting of COC surface allows modification to
47 hydrophilic surface without changing bulk properties, such as optical properties. One of the
48 advantages is the covalent grafted chains offers stable surfaces in contrast to the physical coating
49 which can be delaminated [45]. Modification of COC surface was discussed for different

50 applications, cited in literature like fabrication of smart disposable LOCs for the BIOMEMS
51 applications [45], the bioanalytical applications that require minimal nonspecific adsorption of
52 biomolecules [27], and to increase bond strength of the original surface [43]. However, very few
53 examples are to be found. Li et al. [26] studied the UV-photografting of a hydrophilic
54 polyacrylamide on COC devices in order to reduce protein adsorption and make COC suitable for
55 proteins separations by isoelectric focusing gel electrophoresis. In this example, polyacrylamide
56 grafting was initiated in presence of benzophenone (BP) as photoinitiator. The surface
57 hydrophilicity was characterized by contact angle measurements. Hydrophilicity increased with
58 coating time and for 20 min of UV-irradiation, contact angle measured is $12^\circ - 16^\circ$. PA-coating
59 modified COC surfaces to hydrophilic properties and kept low electroosmotic mobilities. In
60 another example, Du et al. [46] improved the hydrophilicity of COC devices by photografting six
61 acrylates with anionic, neutral and cationic functional groups, to obtain different surface charges.
62 Benzophenone was used as photoinitiator. Influence of irradiation conditions: monomer
63 concentration, reaction temperature, irradiation intensity and time, was followed by contact angle
64 measurements. On COC microchannels modified with 2- acrylamido - 2- methyl -1- propane
65 sulfonic (AMPS) and N-[3-(dimethyl-amino)propyl] methacrylamide, an electrophoretic
66 separation of fluorescein isothiocyanate labeled amino acids was reported. A zwitterionic
67 molecules were successfully grafted by Peng et al. [47] onto the surface of COC microfluidic
68 channels by UV-irradiation of mixed acrylic monomers : 2- acrylamido - 2- methyl -1- propane
69 sulfonic (AMPS) and [2-(acryloyloxy)ethyl]trimethyl ammonium chloride (AETAC). Contact
70 angle showed a modification of COC surface, with BP as photoinitiator, with low angle obtained
71 for ratio AETAC/AMPS = 5.5. These modified COC microchannels showed a highly efficient
72 separation of amino acid, indicating that the surface modification led to a uniform zwitterionic
73 layer.

74 The focus of this work is the surface modification of COC plates, by UV photografting of the
75 hydrophilic monomer: polyethylene glycol diacrylate (PEGDA). For this purpose, an optimisation
76 of PEGDA photografting was investigated by using a central composite design (CCD) in order to
77 obtain a hydrophilic COC surface which enhances anchoring of hexyl acrylate nanoparticle (C_6).
78 Surface morphology was observed by scanning electronic microscopy (SEM) to follow the
79 influence of hydrophilic surface on particles sphericity.

80 **2 Experimental section**

81 **2.1 Materials**

82 All chemicals were supplied by Sigma-Aldrich (Isle – d’Abeau, France) and used as received:
83 sodium dodecyl sulfate (SDS) as surfactant, hexyl acrylate (HA), 2- acrylamide - 2- methyl
84 propane sulfonic acid (AMPS), polyethylene glycol diacrylate (PEGDA 258) as monomers,
85 benzoin methyl ether (BME) as photoinitiator, and pentadecane (C₁₅) as co-stabilizer. Solvents
86 used were acetone and water of Milli-Q grade (resistivity: 18 MΩ).

87 Cyclic olefin copolymer plates (COC, Topas 6013) in format 75.5 mm x 25.5 mm, thickness
88 1.0 mm, were fabricated by Microfluidic Chipchop GmbH (Jena, Germany). These plates were
89 rinsed with acetone and dried under nitrogen before use.

90 **2.2 Hydrophilic monomer PEGDA photografting on COC surface**

91 Hydrophilic monomer PEGDA were mixed to BME and solubilized in acetone under agitation and
92 ultrasound. Aqueous solutions containing different concentrations of PEGDA and BME were
93 tested. BME amount is expressed as weight pourcentage (wt. %) in respect with PEGDA weight
94 or as concentration in water (mol/L). A volume of approximately 500 μL PEGDA-BME mixture
95 was deposited on native COC plate, then enclosed with another COC plate without causing bubbles
96 which could disturbs the polymerization.

97 **2.3 Miniemulsion formulation and polymerisation**

98 Surfactant sodium dodecyl sulfate (SDS) and charged monomer 2- acrylamido - 2- methyl -1-
99 propane sulfonic acid (AMPS) were dissolved in water forming the aqueous phase (φ_{aq}). The
100 organic phase (φ_{org}) was prepared with the monomer hexyl acrylate (HA), the photoinitiator
101 benzoin methyl ether (BME) and the co-stabilizer pentadecane (C₁₅). The composition of the
102 miniemulsion was fixed at 0.1 wt. % SDS and 0.025 wt. % AMPS in the aqueous phase mixed to
103 the organic phase constituted of 5 wt. % HA, 0.35 wt. % C₁₅ and 0.125 wt. % BME. All amounts
104 are expressed in weight percentage (wt. %) with respect to the water weight.

105 Both phases were then mixed in a beaker during 10 min using a magnetic stirrer at 700 rpm leading
106 to an oil-in-water pre-emulsion. This dispersion was then mini-emulsified by ultrasonication with
107 a sonifier (W450 DigitalBranson) at 50% amplitude for 180 s.

108 Miniemulsion was injected between two PEGDA-modified COC plates, and miniemulsion
109 polymerization is performed under irradiation intensity of 2.7 mW/cm^2 for 30 min at $30 \text{ }^\circ\text{C}$. After
110 polymerization, plates are rinsed with deionized water to eliminate non reacted reagents and
111 solvents.

112 **2.4 Characterization of COC surface**

113 2.4.1 Contact angle measurements

114 A droplet of distilled water ($3.3 \text{ }\mu\text{L}$) was dropped off on COC surface at room temperature. The
115 contact angles measured by Digidrop Contact Meter (GBX, Bourg de Péage, France) instrument,
116 are the averages of 15 measurements performed at different locations of the surface.

117 2.4.2 Scanning electron microscopy

118 Morphology of nanoparticles on PEGDA grafted-COC- surfaces were observed by scanning
119 electron microscopy (FEI Quanta FEG 250). Plates were covered with a thin layer (10 - 20 nm) of
120 metal conductor (like platinum or gold-palladium) prior to SEM observations, in order to reduce
121 the charge phenomenon on non-conducting material.

122 **2.5 Optimization design**

123 Surface response methodology as applied to optimize PEGDA photografting in order to obtain a
124 hydrophilic COC surface. The experimental factors studied were the amount of PEGDA (X1),
125 BME (X2) and irradiation time (X3). Others factors were fixed: the solubilization mixture was
126 acetone/water 50/50 (v/v), temperature was fixed at 45°C and intensity of irradiation at
127 2.7 mW/cm^2 . The response Y was the contact angle measured on both plates.

128 A central composite design (CCD) was built with a second-order quadratic equation to model the
129 contact angle (Y1) as follows:

130 $Y = b_0 + b_1X_1 + b_2X_2 + b_3X_3 + b_{12}X_1X_2 + b_{13}X_1X_3 + b_{23}X_2X_3 + b_{11}X_1^2 + b_{22}X_2^2 + b_{33}X_3^2$
 131 (Eq.1)

132 Where Y is the modeled response (Y1), b_0 is the intercept, X_i is the coded factor, b_i is the
 133 corresponding coefficient, b_{ii} is the quadratic coefficient and b_{ij} is the two-factor interaction
 134 coefficient.

135 17 experiments were thus carried out determined by the 2^3 full factorial design with six axial points
 136 at a distance of $\alpha = 1$ from the design center and three center points. The experimental factors and
 137 their levels are given in Table 1.

138 Multiple linear regression, analysis of variance (ANOVA) and residual analysis were performed
 139 with NemrodW®software (LPRAI, Marseille, France).

140

141 **Table 1** Experimental factors and their coded levels in the central composite design, with the corresponding
 142 amounts of PEGDA (mol/L) and BME (wt. % with respect to PEGDA weight) and irradiation time (min).

Level	[PEGDA] (mol/l)	BME (wt. %)	Irradiation time (min)
-1	0.1	1	10
0	0.2	3	15
1	0.3	5	20

143

144 3 Results and discussion

145 Miniemulsion photopolymerization on native COC plates showed a need of surface modification.
 146 Hydrophobic surface of COC seems disturbing miniemulsion stability and therefore, spherical
 147 particles were not anchored. An acrylate layer was obtained. With the view to increasing the
 148 surface coverage, UV-photografting of ionic and neutral monomers was investigated. Firstly,
 149 hydrophobic monomer was tested: ethylene glycol dicyclopentenylether acrylate (DCP). It's a
 150 monomer which has a norbornene group like COC surface, and could be a spacer to anchorage
 151 nanoparticles. This grafting, showed an increase of active sites, but acrylate layers were formed.
 152 Secondly, many hydrophilic monomers were investigated looking for a hydrophilic surface: 2-
 153 acrylamido - 2- methyl -1- propane sulfonic acid (AMPS), 2 (methacryloyloxy)

154 ethyltrimethylammonium chloride (MATEA) and polyethylene glycol diacrylate (PEGDA 258
155 and PEGDA 700). Only PEGDA (258) photografting, showed the anchorage of monodisperse
156 spherical particles. An optimization was studied by experimental design in order to obtain an
157 homogeneous grafting.

158 **3.1 Optimization of PEGDA photografting**

159 Experimental design was built to study the influence of PEGDA concentration, BME amount
160 expressed as percentage in regards to PEGDA weight and irradiation time on surface
161 hydrophilicity by contact angle measurements. PEGDA and BME amounts impact the number and
162 the crosslinking of PEG chains. Furthermore, irradiation time affects the density and the length of
163 PEG chains.

164 Table 2 shows 17 experiments in different conditions, with contact angle measurements as
165 response. Standard deviation, calculated for 15 points in different locations on COC plates,
166 indicates the surface homogeneity of PEGDA grafting. COC plate is considered hydrophilic when
167 contact angle reached a value below 65° . Amongst 17 experiments, only three conditions meet
168 these requirements: test 4, 8 and 12. Test 8 was irradiated for 20 min at the same amounts of
169 PEGDA and BME of test 4, and showed a contact angle slightly superior to the value obtained for
170 the test 4. For test 12, PEGDA grafting was not homogeneous and less reproducible. The low value
171 of contact angle with good homogeneity (59 ± 3) was obtained for experiment 4 for the following
172 conditions: 0.3 M PEGDA, 5 wt. % BME for 10 min of irradiation. The synthesis of nanoparticles
173 on photografted COC plates for these conditions was investigated.

174

175

176

177

178

179

180

181

182

183

184

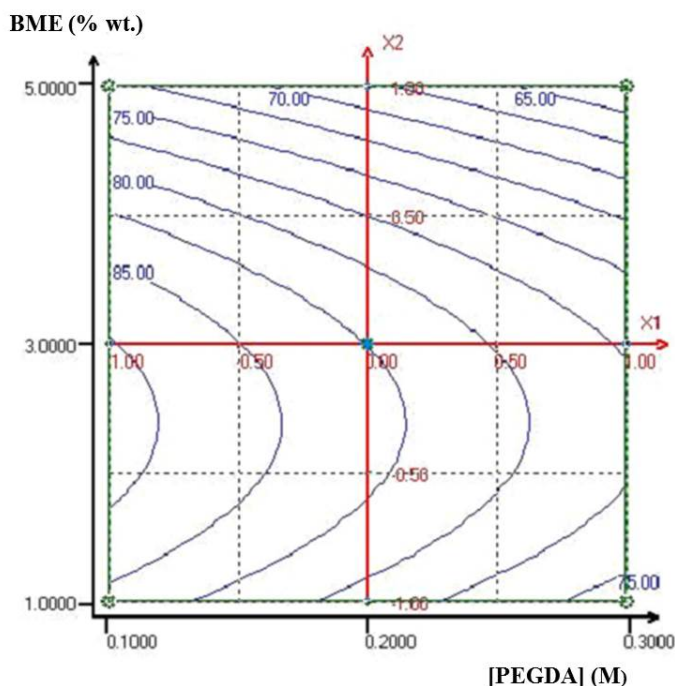
185

186 **Table 2** Three-factor central composite design with corresponding response: contact angle measurements
 187 \pm standard deviation. The amount of BME is express in weight percent with respect to PEGDA weight.

Experiments	[PEGDA] (M)	wt. % BME	Irradiation time (min)	Contact angle ($^{\circ}$) \pm standard deviation
1	0.10	1	10	83 \pm 3
				85 \pm 1
2	0.30	1	10	71 \pm 6
				70 \pm 6
3	0.10	5	10	78 \pm 4
				76 \pm 4
4	0.30	5	10	59 \pm 3
				59 \pm 3
5	0.10	1	20	84 \pm 6
				84 \pm 7
6	0.30	1	20	69 \pm 5
				72 \pm 5
7	0.10	5	20	74 \pm 9
				73 \pm 5
8	0.30	5	20	65 \pm 4
				65 \pm 7
9	0.10	3	15	79 \pm 5
				80 \pm 3
10	0.30	3	15	78 \pm 7
				81 \pm 5
11	0.20	1	15	84 \pm 2
				85 \pm 1
12	0.20	5	15	61 \pm 8
				67 \pm 9
13	0.20	3	10	85 \pm 3
				81 \pm 3
14	0.20	3	20	77 \pm 5
				78 \pm 4
15	0.20	3	15	87 \pm 2
				85 \pm 3

16	0.20	3	15	81 ± 6
				84 ± 8
17	0.20	3	15	77 ± 6
				73 ± 7

188



189

190 **Figure 1** : Contour plot of contact angle for 10 min of irradiation.

191

192 The results shown in Table 2 for 17 experiments done in different conditions were analyzed by a
 193 contour plot. This plot (Figure 4) allows the determination of PEGDA and BME concentrations
 194 leading to hydrophilic surface after photopolymerization during a specific irradiation time.
 195 Contour plots for different irradiation time tested were similar, so irradiation time has no influence
 196 on the response. Therefore, 10 min of irradiation was fixed. The plot also revealed a decrease of
 197 contact angle values, so an increase of hydrophilicity for high amounts of PEGDA (0.3 M) and
 198 BME (5 wt. %).

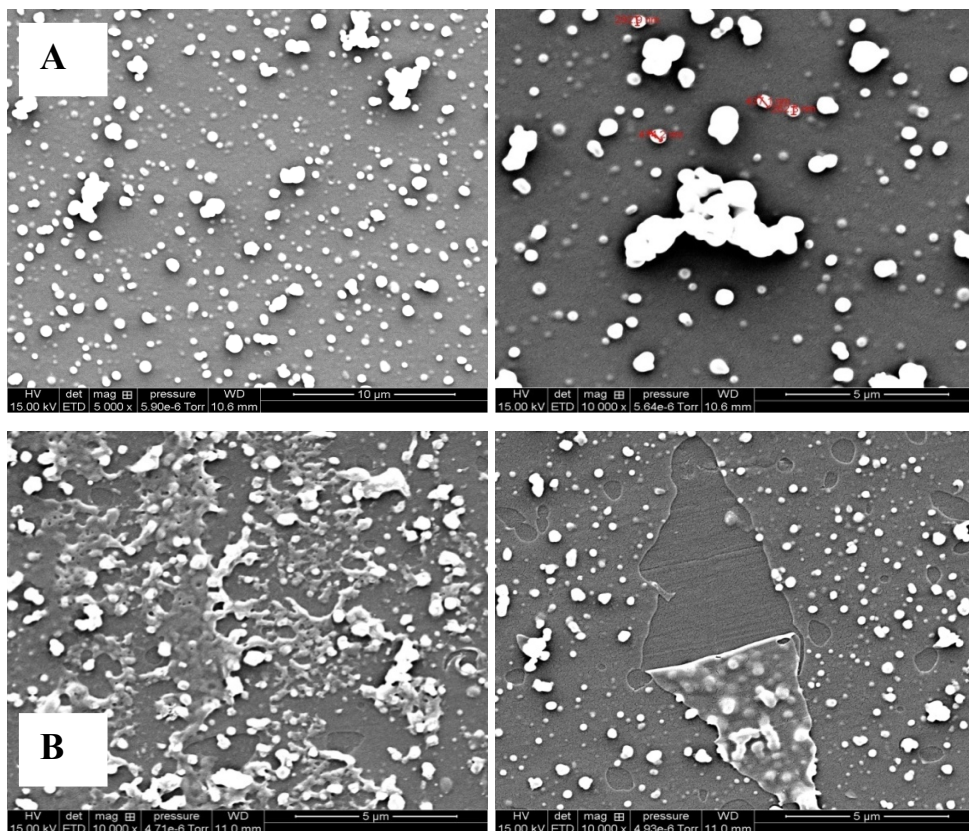
199 3.2 Increase of PEGDA concentration

200 In order to enhance the hydrophilic character of COC plates, an increase of PEGDA concentration
 201 might increase the anchorage of PEG chains which makes surface hydrophilic. Experiments with
 202 higher amount of PEGDA (0.4 M and 0.5 M) at 5 wt. % BME, were tested. For 0.4 M PEGDA

203 concentration, contact angle measured was $56^\circ \pm 4$. Photografting in these conditions was found
204 to be not repeatable; other COC-PEGDA plates presented a contact angle of $73^\circ \pm 3$. For 0.5 M
205 PEGDA, the surface was hydrophilic with contact angle of $64^\circ \pm 4$. Nanoparticles on COC-
206 PEGDA plates for both photografting conditions were then observed by scanning electronic
207 microscopy (Figure 2).

208

209



210

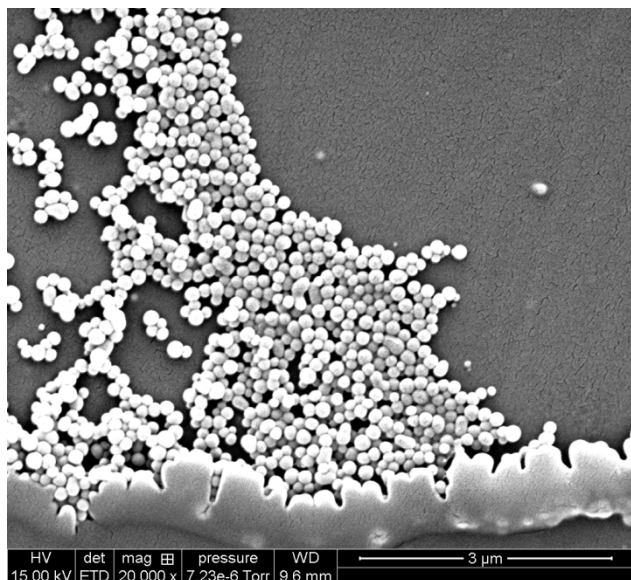
211

212 **Figure 2** SEM Images **A** : 0.4 M PEGDA + 5 % wt. BME in water/acetone 50/50 (v/v); 10 min, 45°C,
213 2.7 mW/cm². MEB x 5000, x 10000. **B** : 0.5 M PEGDA + 5 % wt. BME in water/acetone 50/50 (v/v);
214 10 min, 45°C, 2.7 mW/cm². MEB x 10000. Miniemulsion photopolymerization: 30 min, 30°C,
215 2.7 mW/cm². Tension 15 kV.

216

217 For 0.4 M PEGDA (Figure 2A) particles are merged and distorted. Acrylate layer, which is not
218 stable and peels off, was further observed for 0.5 M PEGDA (Figure 2B). To overcome these
219 problems, PEGDA concentration was fixed at 0.3 M with 5 wt. % of BME. For these conditions,
220 PEGDA-grafted COC plate contact angle was measured between 60° and 65° (Figure 1). The

221 synthesis of nanoparticles on the modified COC plates using this protocol (0.3 M PEGDA and
222 5 % wt. BME) was characterized by SEM observations (Figure 3).



224 **Figure 3** SEM image for nanoparticles on modified COC plate. PEGDA photografting : 0.3 M
225 PEGDA + 5 % wt. BME in water/acetone 50/50 (v/v) ; 10 min, 45°C, 2.7 mW/cm². Miniemulsion
226 photopolymerization: 30 min, 30°C, 2.7 mW/cm². MEB x 20000. Tension 15 kV.
227

228 Anchorage of spherical nanoparticles is unfortunately not sufficient and not homogeneous on COC
229 (Figure 3). It seems that PEG chains are not grafted on the surface because of the amount of BME
230 which might be insufficient to create active sites on COC by hydrogen abstraction. BME amount
231 impact PEGDA grafting, but furthermore number of active sites on COC surface. Therefore,
232 influence of BME was investigated by concentration.

233 3.3 Influence of BME concentration

234 Influence of BME amount on hydrophilicity COC surface was studied in percent in respect to
235 PEGDA weight to initiate reticulation of PEG chains and form a compact polymeric layer.
236 Furthermore, BME could act on COC surface by hydrogen abstraction, and therefore, it would be
237 interesting to analyse with another point of view the influence of the photoinitiator by controlling
238 BME concentration (mM) in regards to the polymerization mixture. This concentration should be
239 optimized in order to promote a large number of active sites and enhance anchorage of

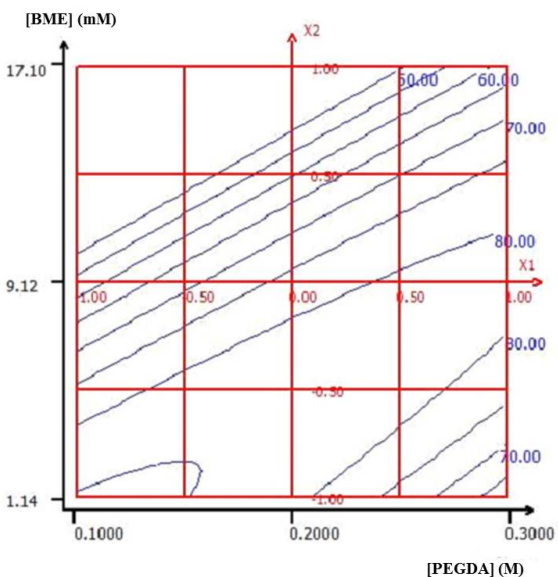
240 nanoparticles. BME concentrations are mentioned in Table 3 , and the contour plot according to
241 BME and PEGDA concentration is represented in Figure 4.

242

243 **Table 3** Experimental design expressed with BME concentration (mM)

Experiments	PEGDA Concentration (M)	% wt. BME	BME concentration (mM)	Irradiation time (min)	Y1 : Contact angle average (°)
1	0.10	1	1.14	10	84
2	0.30	1	3.42	10	71
3	0.10	5	5.70	10	76
4	0.30	5	17.10	10	59
5	0.10	1	1.14	20	84
6	0.30	1	3.42	20	71
7	0.10	5	5.70	20	73
8	0.30	5	17.10	20	65
9	0.10	3	3.42	15	79
10	0.30	3	10.26	15	80
11	0.20	1	2.28	15	84
12	0.20	5	11.40	15	64
13	0.20	3	6.84	10	83
14	0.20	3	6.84	20	78
15	0.20	3	6.84	15	86
16	0.20	3	6.84	15	82
17	0.20	3	6.84	15	75

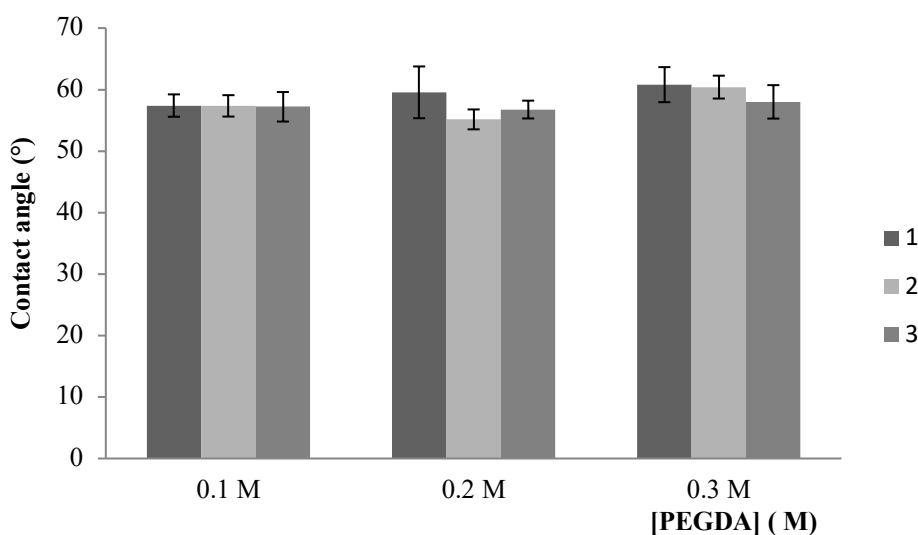
244



245

246 **Figure 4** Contour plot of contact angle for 10 min of irradiation according to BME and PEGDA
 247 concentration.

248 BME, by hydrogen abstraction, forms more active sites on the surface, which promote anchorage
 249 of PEG chains. Contour plot of contact angle represented in Figure 4, indicated a hydrophilic
 250 character for higher BME concentration. Thereby, the hypothesis is verified. For 17 mM BME,
 251 which is the maximum concentration that was tested, contact angle is between 50° and 60° for
 252 various PEGDA concentrations (0.1 M – 0.3 M). For these conditions, reproducibility of PEGDA
 253 photografting was verified by three measures of contact angle (Figure 5).



254

255 **Figure 5** Reproducibility chart of PEGDA photografting. Contact angle ($^{\circ}$) according to PEGDA
256 concentration (M) for 17 mM BME. Photopolymerization 10 min, 45°C, 2.7 mW/cm².

257

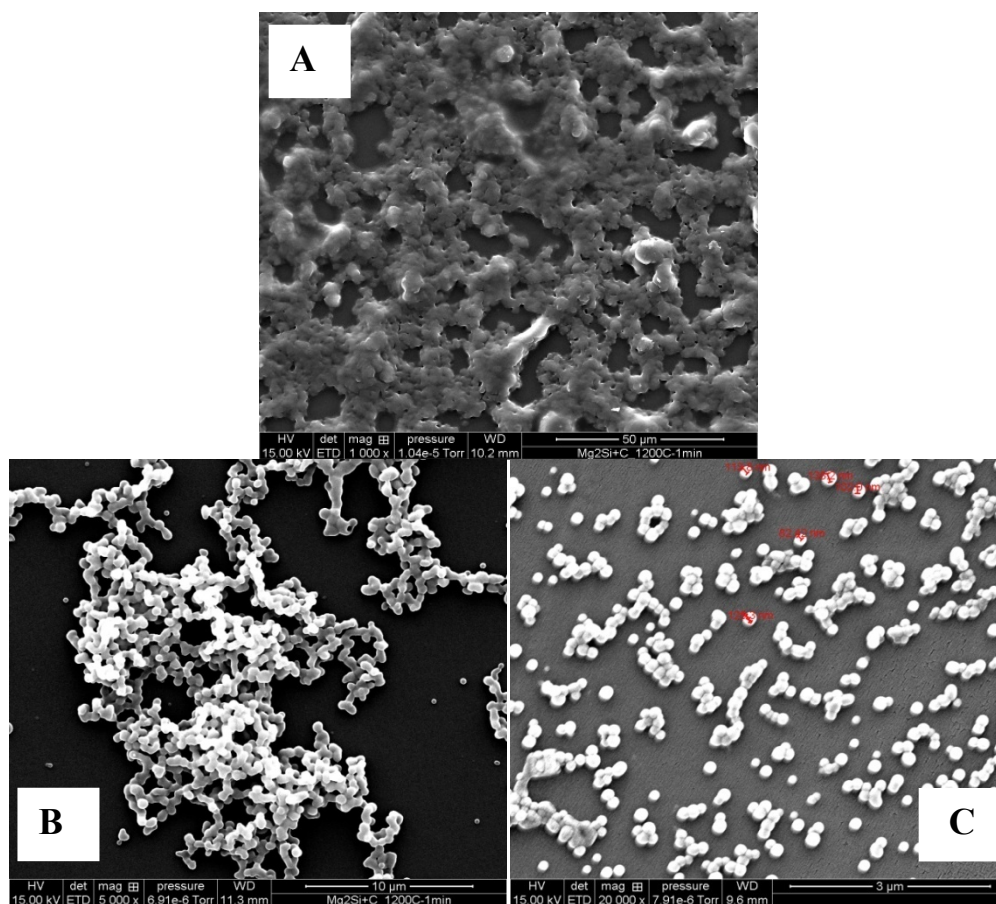
258 To follow the impact of BME and PEGDA concentration on the sphericity of particles,
259 UV-synthesis of acrylate particles on PEGDA-modified COC plates with 17 mM BME and
260 PEGDA concentrations between 0.1 M and 0.3 M were performed. Figure 6 represent
261 morphologies of the resulting particles.

262

263

264

265



266

267

268 **Figure 6** SEM Images of nanoparticles anchored on PEGDA-modified COC- surfaces. PEGDA
269 photopolymerization with 17 mM BME, 10 min, 45°C, 2.7 mW/cm. **A** : 0.1 M, MEB X 1000. **B** : 0.2 M,

270 MEB X 5000. C : 0.3 M PEGDA concentration, respectively, MEB X 20000. Miniemulsion
271 photopolymerization: 30 min, 30°C, 2.7 mW/cm². Tension 15 kV.

272 Figure 6A represent nanoparticles synthesis on modified COC with low concentration of PEGDA
273 (0.1 M). Contact angle measured was between 55° and 65°. SEM morphologies, showed a fusion
274 of particles on the surface. Low amount of PEGDA consumes a part of BME and the excess will
275 form free radicals by hydrogen abstraction from COC. The non-grafted COC surface by PEG
276 chains seems to destabilize miniemulsion due to his hydrophobic nature. For higher concentration
277 of PEGDA, nanoparticles become more spherical with diameter between
278 80 nm and 140 nm for 0.3 M PEGDA (Figure 6C). These results verified that low PEGDA
279 concentration, is not sufficient to consume BME and form spherical nanoparticles. Monodisperse
280 hexyl acrylate nanoparticles with diameter inferior to 200 nm are obtained for 0.3 M PEGDA at
281 17 mM BME, which is in accordance to the specifications.

282 Unfortunately, these irradiation conditions were not compatible with COC chips. A concentration
283 of 0.3 M PEGDA is considered too elevated for the surface modification to be implemented in
284 microchannels, as it oftenly leads to channel blockage. To overcome this problem, we extended
285 our study for PEGDA concentration field between 0.05 M and 0.2 M.

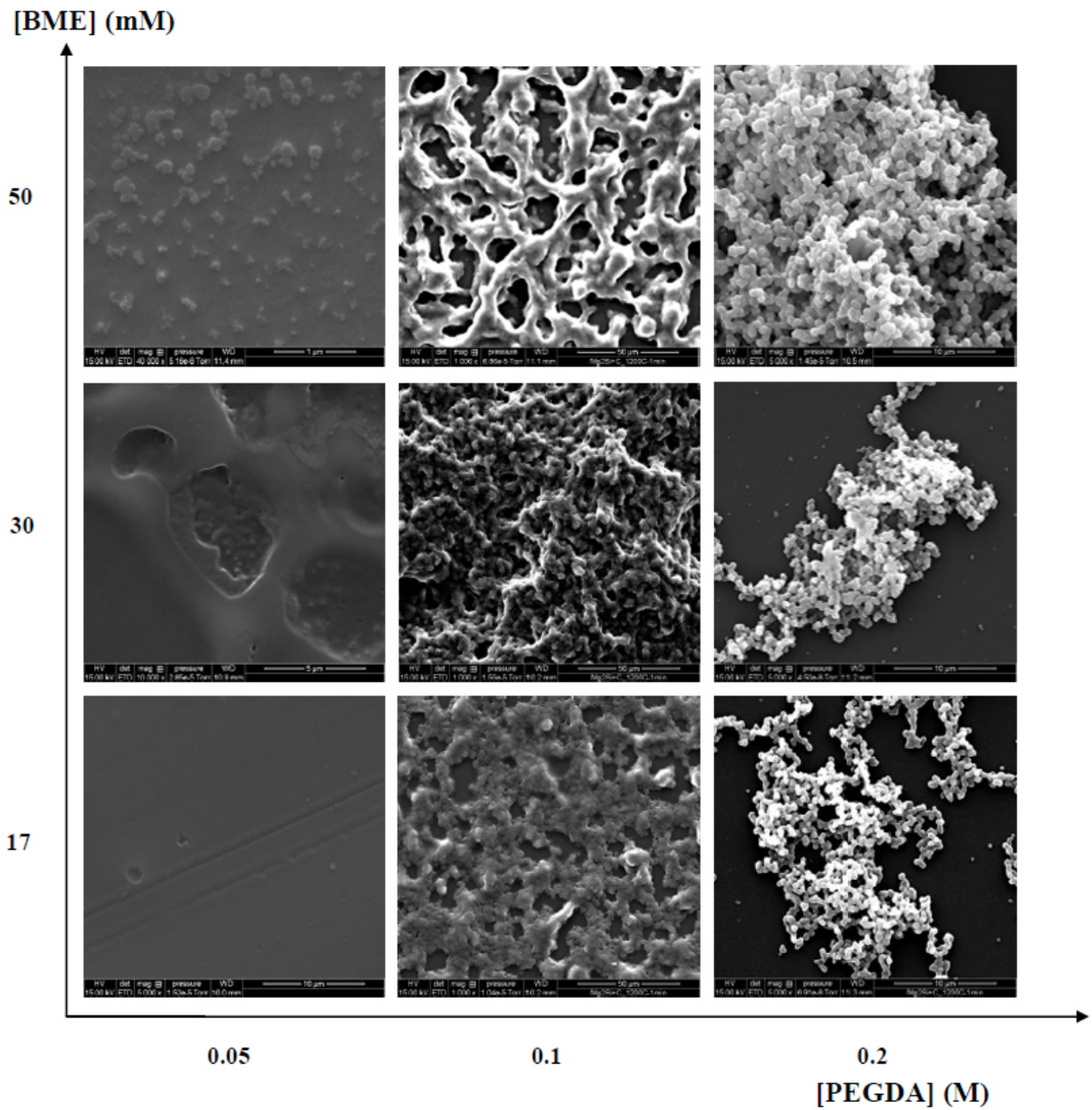
286 **3.4 UV-Synthesis of nanoparticles on modified COC plates**

287 Anchorage of nanoparticles on COC-PEGDA surfaces depends on polymerization conditions. For
288 different synthesis on modified COC substrates, morphologies of nanoparticles were followed by
289 SEM images. PEGDA photografting was explored for various PEGDA concentrations: 0.05 M,
290 0.1 M and 0.2 M with BME concentrations reaching 17 mM, 30 mM and 50 mM (Figure 7). BME
291 concentration impacts the number of PEGDA chains grafted. At higher concentration an increase
292 of the number of PEGDA chains can be observed. Otherwise, an excess of non-reacted BME can
293 interfere with COC surface.

294 On the first hand, the diagram is interpreted in a horizontal manner. For a fixed value of BME
295 concentration, no particles were observed at 0.05 M and 0.1 M PEGDA. Particles are fusion and
296 leads to an acrylate monolayer. PEGDA concentrations seem insufficient to consume BME even
297 at low concentration of 17 mM. Therefore, the miniemulsion was not stable in contact with the
298 surface, as previously observed. At 0.2 M PEGDA, SEM images showed spherical particles
299 anchored on COC surface. On the other hand, a vertical analysis of Figure 10 showed that more

300 particles distortion and acrylate layers happened for 0.05 M and 0.1 M PEGDA at higher
301 concentrations of BME. This might be due to the excess of BME non-reacted. For PEGDA
302 concentration higher than 0.2 M with higher concentration of BME more active sites were formed.
303 Thus, the number of spherical particles on the surface was enhanced.

304 In conclusion, PEGDA and BME amounts not only impact the hydrophilicity nature of COC but
305 also the sphericity of nanoparticles anchored. The increase of BME concentration leads to an
306 increase of active sites occupied then by PEGDA at higher concentrations. Therefore an increase
307 of number of spherical nanoparticles on the surface is observed. 0.2 M PEGDA at 30 mM BME
308 respond to the specification.



309

310 **Figure 7** SEM Images of nanoparticles anchored on modified COC surfaces by different PEGDA and
 311 BME concentrations. Photopolymerization: 10 min, 45°C, 2.7 mW/cm. Miniemulsion
 312 photopolymerization: 30 min, 30°C, 2.7 mW/cm². Tension 15 kV.

313

314

315

316 **4 Conclusion**

317 The anchorage of hexyl acrylate nanoparticles on COC surface requires a surface modification
318 from hydrophobic to hydrophilic nature. This study studied the optimization of PEGDA
319 photografting by using response surface methodology as regard to PEGDA and BME amounts and
320 irradiation time. A large experimental field has been explored using water contact angle
321 measurement which indicates the hydrophobic/hydrophilic nature of the substrate. COC surface
322 has been considered sufficiently hydrophilic for a contact angle inferior to 65°. The hydrophilic
323 PEGDA-modified COC surface promotes anchorage of nanoparticles, as observed by SEM
324 images. Both PEGDA and BME concentrations used during the first surface modification step
325 impact the anchorage of nanoparticules that occurs during in-situ photopolymerization as well as
326 the morphology of the resulting particles. A compromise between PEGDA and BME amount
327 should be made to maintain spherical particles sufficiently anchored on COC plates and
328 microchips. Synthesis of nanoparticles on modified COC plates grafted with PEGDA was
329 achieved. An optimization of polymerization conditions in COC microchips should be done to
330 avoid plugging channels and to develop a novel stationary phase which could be used in
331 electrochromatography.

332 **Acknowledgements**

333 The authors acknowledge the financial support by French National Research Agency (ANR)
334 through Nanochrom project (11-JS09-017-01).

335

336

337

338

339

340

341

342

343 **References**

- 344 1. Knox, J.H. and M. Saleem, *Kinetic Conditions for Optimum Speed and Resolution in*
345 *Column Chromatography*. Journal of Chromatographic Science, 1969. **7**(10): p. 614-622.
- 346 2. Knox, J.H., *Practical Aspects of LC Theory*. Journal of Chromatographic Science, 1977.
347 **15**(9): p. 352-364.
- 348 3. Desmet, G., D. Clicq, and P. Gzil, *Geometry-Independent Plate Height Representation*
349 *Methods for the Direct Comparison of the Kinetic Performance of LC Supports with a*
350 *Different Size or Morphology*. Analytical Chemistry, 2005. **77**(13): p. 4058-4070.
- 351 4. Nguyen, D.T.T., et al., *Chromatographic behaviour and comparison of column packed*
352 *with sub-2 μm stationary phases in liquid chromatography*. Journal of Chromatography
353 A, 2006. **1128**(1-2): p. 105-113.
- 354 5. Nguyen, D.T.T., et al., *Fast analysis in liquid chromatography using small particle size*
355 *and high pressure*. Journal of Separation Science, 2006. **29**(12): p. 1836-1848.
- 356 6. Kundu, P., et al., *Stability of oil-in-water macro-emulsion with anionic surfactant: Effect*
357 *of electrolytes and temperature*. Chemical Engineering Science, 2013. **102**(0): p. 176-
358 185.
- 359 7. Chemtob, A., et al., *Photoinduced miniemulsion polymerization*. Colloid and Polymer
360 Science, 2010. **288**(5): p. 579-587.
- 361 8. Hoijemberg, P.A., A. Chemtob, and C. Croutxé-Barghorn, *Two Routes Towards*
362 *Photoinitiator-Free Photopolymerization in Miniemulsion: Acrylate Self-Initiation and*
363 *Photoactive Surfactant*. Macromolecular Chemistry and Physics, 2011. **212**(22): p. 2417-
364 2422.
- 365 9. Saadé, J., et al., *Response surface optimization of miniemulsion: application to UV*
366 *synthesis of hexyl acrylate nanoparticles*. Colloid and Polymer Science, 2015. **294**(1): p.
367 27-36.
- 368 10. Yang, W. and B. Rånby, *Radical Living Graft Polymerization on the Surface of*
369 *Polymeric Materials*. Macromolecules, 1996. **29**(9): p. 3308-3310.
- 370 11. Ma, Y., L. Liu, and W. Yang, *Photo-induced living/controlled surface radical grafting*
371 *polymerization and its application in fabricating 3-D micro-architectures on the surface*
372 *of flat/particulate organic substrates*. Polymer, 2011. **52**(19): p. 4159-4173.
- 373 12. Ma, H., R.H. Davis, and C.N. Bowman, *A Novel Sequential Photoinduced Living Graft*
374 *Polymerization*. Macromolecules, 1999. **33**(2): p. 331-335.
- 375 13. Zhao, C., Z. Zhang, and W. Yang, *A remote photochemical reaction for surface*
376 *modification of polymeric substrate*. Journal of Polymer Science Part A: Polymer
377 Chemistry, 2012. **50**(18): p. 3698-3702.
- 378 14. Schneider, M.H., Y. Tran, and P. Tabeling, *Benzophenone Absorption and Diffusion in*
379 *Poly(dimethylsiloxane) and Its Role in Graft Photo-polymerization for Surface*
380 *Modification*. Langmuir, 2011. **27**(3): p. 1232-1240.
- 381 15. Ladner, Y., et al., *New "one-step" method for the simultaneous synthesis and anchoring*
382 *of organic monolith inside COC microchip channels*. Lab on a Chip, 2012. **12**(9): p.
383 1680-1685.
- 384 16. Wang, Y. and W. Yang, *MMA/DVB Emulsion Surface Graft Polymerization Initiated by*
385 *UV Light*. Langmuir, 2004. **20**(15): p. 6225-6231.

- 386 17. Wang, Y., et al., *Directly Fabricating Monolayer Nanoparticles on a Polymer Surface by*
387 *UV-Induced MMA/DVB Microemulsion Graft Polymerization*. *Macromolecular Rapid*
388 *Communications*, 2005. **26**(2): p. 87-92.
- 389 18. Gustafsson, O., K.B. Mogensen, and J.P. Kutter, *Underivatized cyclic olefin copolymer*
390 *as substrate material and stationary phase for capillary and microchip*
391 *electrochromatography*. *ELECTROPHORESIS*, 2008. **29**(15): p. 3145-3152.
- 392 19. Rohr, T., et al., *Surface Functionalization of Thermoplastic Polymers for the Fabrication*
393 *of Microfluidic Devices by Photoinitiated Grafting*. *Advanced Functional Materials*,
394 2003. **13**(4): p. 264-270.
- 395 20. Kumlangdudsana, P., S.T. Dubas, and a.L. Dubas, *Surface Modification of Microfluidic*
396 *Devices*. *Journal of Metals, Materials and Minerals.*, 2007. **17** (2): p. 67-74.
- 397 21. Roy, S., et al., *Surface analysis, hydrophilic enhancement, ageing behavior and flow in*
398 *plasma modified cyclic olefin copolymer (COC)-based microfluidic devices*. *Sensors and*
399 *Actuators B: Chemical*, 2010. **150**(2): p. 537-549.
- 400 22. Roy, S. and C.Y. Yue, *Surface Modification of COC Microfluidic Devices: A*
401 *Comparative Study of Nitrogen Plasma Treatment and its Advantages Over Argon and*
402 *Oxygen Plasma Treatments*. *Plasma Processes and Polymers*, 2011. **8**(5): p. 432-443.
- 403 23. Tsao, C.W., et al., *Low temperature bonding of PMMA and COC microfluidic substrates*
404 *using UV/ozone surface treatment*. *Lab on a Chip*, 2007. **7**(4): p. 499-505.
- 405 24. Zhang, J., C. Das, and Z.H. Fan, *Dynamic coating for protein separation in cyclic olefin*
406 *copolymer microfluidic devices*. *Microfluidics and Nanofluidics*, 2008. **5**(3): p. 327-335.
- 407 25. Brisset, F., et al., *Surface functionalization of cyclic olefin copolymer with aryldiazonium*
408 *salts: A covalent grafting method*. *Applied Surface Science*, 2015. **329**(0): p. 337-346.
- 409 26. Li, C., et al., *Isoelectric focusing in cyclic olefin copolymer microfluidic channels coated*
410 *by polyacrylamide using a UV photografting method*. *Electrophoresis*, 2005. **26**(9): p.
411 1800-6.
- 412 27. Stachowiak, T.B., et al., *Hydrophilic surface modification of cyclic olefin copolymer*
413 *microfluidic chips using sequential photografting*. *J Sep Sci*, 2007. **30**(7): p. 1088-93.
- 414 28. Hu, S., et al., *Surface-Directed, Graft Polymerization within Microfluidic Channels*.
415 *Analytical Chemistry*, 2004. **76**(7): p. 1865-1870.
- 416 29. Burke, J.M. and E. Smela, *A novel surface modification technique for forming porous*
417 *polymer monoliths in poly(dimethylsiloxane)*, in *Biomicrofluidics*. 2012: United States. p.
418 16506-1650610.
- 419 30. Almutairi, Z., C.L. Ren, and L. Simon, *Evaluation of polydimethylsiloxane (PDMS)*
420 *surface modification approaches for microfluidic applications*. *Colloids and Surfaces A:*
421 *Physicochemical and Engineering Aspects*, 2012. **415**(0): p. 406-412.
- 422 31. Stachowiak, T.B., F. Svec, and J.M.J. Fréchet, *Patternable Protein Resistant Surfaces for*
423 *Multifunctional Microfluidic Devices via Surface Hydrophilization of Porous Polymer*
424 *Monoliths Using Photografting*. *Chemistry of Materials*, 2006. **18**(25): p. 5950-5957.
- 425 32. Kholdi, O.E., et al., *Modification of adhesive properties of a polyethylene film by*
426 *photografting* *Journal of Applied Polymer Science Volume 92, Issue 5*. *Journal of*
427 *Applied Polymer Science*, 2004. **92**(5): p. 2803-2811.
- 428 33. Wang, H. and H.R. Brown, *Ultraviolet grafting of methacrylic acid and acrylic acid on*
429 *high-density polyethylene in different solvents and the wettability of grafted high-density*
430 *polyethylene. I. Grafting*. *Journal of Polymer Science Part A: Polymer Chemistry*, 2004.
431 **42**(2): p. 253-262.

- 432 34. Li, G., et al., *Surface photografting initiated by benzophenone in water and mixed*
433 *solvents containing water and ethanol*. Journal of Applied Polymer Science, 2012.
434 **123**(4): p. 1951-1959.
- 435 35. Yang, W. and B. Rånby, *Bulk surface photografting process and its applications. II.*
436 *Principal factors affecting surface photografting*. Journal of Applied Polymer Science,
437 1996. **62**(3): p. 545-555.
- 438 36. Decker, C. and K. Zahouily, *Surface modification of polyolefins by photografting of*
439 *acrylic monomers*. Macromolecular Symposia, 1998. **129**(1): p. 99-108.
- 440 37. Wang, Y., et al., *Facile Surface Superhydrophilic Modification: NVP/MBA Inverse*
441 *Microemulsion Surface-Grafting Polymerization Initiated by UV Light*. Macromolecular
442 Rapid Communications, 2005. **26**(22): p. 1788-1793.
- 443 38. He, D. and M. Ulbricht, *Surface-selective photo-grafting on porous polymer membranes*
444 *via a synergist immobilization method*. Journal of Materials Chemistry, 2006. **16**(19): p.
445 1860-1868.
- 446 39. Balart, J., et al., *Surface modification of polypropylene substrates by UV photografting of*
447 *methyl methacrylate (MMA) for improved surface wettability*. Journal of Materials
448 Science, 2012. **47**(5): p. 2375-2383.
- 449 40. Ma, H., R.H. Davis, and C.N. Bowman, *Principal factors affecting sequential*
450 *photoinduced graft polymerization*. Polymer, 2001. **42**(20): p. 8333-8338.
- 451 41. Feng, Y., et al., *Grafting of poly(ethylene glycol) monoacrylates on*
452 *polycarbonateurethane by UV initiated polymerization for improving hemocompatibility*.
453 Journal of Materials Science: Materials in Medicine, 2013. **24**(1): p. 61-70.
- 454 42. Stachowiak, T.B., et al., *Fabrication of porous polymer monoliths covalently attached to*
455 *the walls of channels in plastic microdevices*. Electrophoresis, 2003. **24**(21): p. 3689-
456 3693.
- 457 43. Jena, R.K., C.Y. Yue, and L. Anand, *Improvement of thermal bond strength and surface*
458 *properties of Cyclic Olefin Copolymer (COC) based microfluidic device using the photo-*
459 *grafting technique*. Sensors and Actuators B: Chemical, 2011. **157**(2): p. 518-526.
- 460 44. Roy, S., et al., *Low-temperature (below T_g) thermal bonding of COC microfluidic*
461 *devices using UV photografted HEMA-modified substrates: high strength, stable*
462 *hydrophilic, biocompatible surfaces*. Journal of Materials Chemistry, 2011. **21**(38): p.
463 15031-15040.
- 464 45. Roy, S., et al., *Fabrication of smart COC chips: Advantages of N-vinylpyrrolidone (NVP)*
465 *monomer over other hydrophilic monomers*. Sensors and Actuators B: Chemical, 2013.
466 **178**(0): p. 86-95.
- 467 46. Du, G., et al., *In-channel tuning of hydrophilicity and surface charge of cyclic olefin*
468 *copolymer microchips by UV-induced graft polymerization and its application in lab-on-*
469 *a-chip devices*. Chemical Engineering Journal, 2012. **195–196**(0): p. 132-139.
- 470 47. Peng, X., et al., *Charge Tunable Zwitterionic Polyampholyte Layers Formed in Cyclic*
471 *Olefin Copolymer Microchannels through Photochemical Graft Polymerization*. ACS
472 Applied Materials & Interfaces, 2013. **5**(3): p. 1017-1023.

473

474